Finite-Element Formalism for Nonlinear Slab-Guided Waves

KAZUYA HAYATA, MICHIO NAGAI, AND MASANORI KOSHIBA, SENIOR MEMBER, IEEE

Abstract—**A unified computer-aided numerical approach based on the finite-element method is developed for analyzing optical waves guided by dielectric slab waveguiding structures with arbitrary nonlinear media. In the formulations, both TE and TM polarizations are considered. For the TM case, the biaxial nature of nonlinear refractive index is considered without any approximation. Numerical results are presented for nonlinear TE and TM waves propagating in symmetric slab waveguides. The dependence of dispersion relations on the refractive-index profile of the film is also examined.**

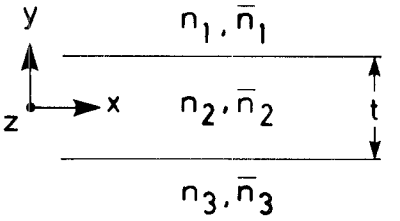

Fig. 1. Nonlinear slab waveguide and coordinate system.

I. INTRODUCTION

THE PROPERTIES of nonlinear optical waves guided by dielectric thin films are of great interest because of their unique features and their potential use in all-optical signal processing devices, such as bistability, switching, and upper and lower threshold devices and optical limiters [1]–[6]. These applications have recently stimulated more practical theoretical investigations of the behavior of the nonlinear guided waves [7]–[28].

The representative methodology for studying these waves propagating in a dielectric slab geometry has been to solve nonlinear wave equations analytically [2]–[5]. Although in this approach exact solutions are obtainable by solving a transcendental equation, it is applicable only to the TE-polarized (*s*-polarized) waves propagating in media with Kerr-like nonlinearity. Thus, if one wants to deal with non-Kerr-like nonlinearity [15], [18], which is frequently encountered in realistic situations, and TM-polarized (*p*-polarized) waves [7], [9], [12], [13], [23], [25], [26], it is necessary either to rely on unrealistic approximate procedures or to solve the problem numerically. To date, the main method has been the former. Only recently, attempts for the latter have been made using the first integral of the nonlinear wave equation [10], [18], the beam-propagation method [17], [20], and the multilayer approximation [22], all of which have been restricted to the case of TE polarization. Although the TM polarization problem has recently been discussed quite extensively in a few approximate ways [7] [9], [12], [13], [25], [26], very few numerical calculations have actually been carried out for dielectric slab configurations. This is due to the fact that the wave equation of the TM mode is considerably more difficult to treat than its TE counterpart and the nonlinear material exhibits the biaxial nature of the refractive index [4], [23], because the TM mode necessarily involves two nonzero electric-field components.

In this paper, to analyze systematically the stationary mode characteristics of optical waves guided by dielectric slab waveguides with arbitrary nonlinear media and with arbitrary refractive-index distribution, a unified numerical approach based on the finite-element technique is developed for both TE and TM waves. For the TM case, the biaxial nature of the nonlinear refractive index is considered without any approximation. In this approach, self-consistent solutions are obtainable via a simple iterative scheme. Furthermore, if one wants to accelerate the convergence speed, it is also possible to apply a skillfull technique such as the Aitken method. Numerical results are presented for nonlinear TE and TM waves guided by symmetric slab waveguiding configurations bounded by two identical nonlinear claddings, and several fascinating features that have not yet been found are shown in a comprehensive way. The dependence of dispersion characteristics on the refractive-index distribution of the film is also investigated in some detail.

II. FINITE-ELEMENT FORMALISM

The geometry under consideration is shown in Fig. 1, where t is the thickness of the film, n_i the linear (low-power) refractive index, and $\bar{n}_i$ the nonlinear optical coefficient ($i = 1, 2, 3$). For self-focusing action $\bar{n}_i > 0$, whereas for self-defocusing action $\bar{n}_i < 0$. We assume that the waveguide is composed of loss-free media and $\partial/\partial x \equiv 0$.

Manuscript received December 14, 1987; revised February 22, 1988. This work was supported in part by Joint Research for Large-Scale Computations Using Vector Processors, Hokkaido University Computing Center, Sapporo, Japan.

The authors are with the Department of Electronic Engineering, Hokkaido University, Sapporo, 060, Japan.

IEEE Log Number 8821224.

0018-9480/88/0700-1207$01.00 ©1988 IEEE

A. TE Waves (S-Polarized Waves)

We consider the following nonlinear relative permittivity ϵ_x' for TE polarization:

$$\epsilon_x' = \epsilon + af(E_x) \tag{1a}$$

$$a = c_0\epsilon_0\varepsilon\bar{n}, \qquad \epsilon = n^2 \tag{1b}$$

where c_0 is the velocity of light in a vacuum ($c_0 = 3.00\times10^8$ m/s), ϵ_0 the vacuum permittivity ($\epsilon_0 = 8.85\times10^{-12}$ F/m), and $f(E_x)$ a function representing flux-dependent permittivity of nonlinear media. For the well-known Kerr-type nonlinearity, $f(E_x) = |E_x|^2$.

Substituting (1a) into Maxwell's equations, the following nonlinear Helmholtz-type equation is derived:

$$\frac{d^2E_x}{dy^2} + \left(k_0^2\epsilon_x' - \beta^2\right)E_x = 0 \tag{2}$$

where k_0 is the free-space wavenumber, β the phase constant, and the wave factor $\exp\{j(\omega t - \beta z)\}$ is implied, where ω is the angular frequency.

Dividing the cross section along the y axis of the guide ($y \geqslant 0$) into a number of second-order line elements, the normalized electric fields within each element are defined in terms of those at the nodal points:

$$\bar{E}_x = \{N\}^T\{\bar{E}_x\}_e \tag{3a}$$

where

$$\{N\} = [N_1 \quad N_2 \quad N_3]^T \tag{3b}$$

$$N_1 = L_1(2L_1 - 1) \qquad N_2 = L_2(2L_2 - 1)$$

$$N_3 = 4L_1L_2 \tag{3c}$$

$$L_1 = (y_2 - y)/l \qquad L_2 = (y - y_1)/l,$$

$$l = y_2 - y_1 \tag{3d}$$

$$\{\bar{E}_x\}_e = \left[\bar{E}_{x,1} \quad \bar{E}_{x,2} \quad \bar{E}_{x,3}\right]^T. \tag{3e}$$

Here $\{N\}$ is the shape function vector, T a transpose, and $\{\bar{E}_x\}_e$ an electric field vector corresponding to the nodal points within each element.

Using Galerkin's procedure on a normalized version of (2) and integrating by parts, we obtain

$$\{N\}\frac{d\bar{E}_x}{dy}\bigg|_{y=y_1}^{y=y_2} - \int_{y_1}^{y_2}\frac{d\{N\}}{dy}\frac{d\bar{E}_x}{dy}\,dy + k_0^2\int_{y_1}^{y_2}\epsilon_x'\{N\}\bar{E}_x\,dy - \beta^2\int_{y_1}^{y_2}\{N\}\bar{E}_x\,dy = \{0\} \tag{4}$$

where $\{0\}$ is a null vector (3×1).

Substituting (3a) into (4) and assembling the complete matrices for the system by adding the contributions of all different elements, we obtain

$$[K(E_x)]\{\bar{E}_x\} - (\beta/k_0)^2[M]\{\bar{E}_x\} = \{0\} \tag{5a}$$

$$[K(E_x)] = \sum_e\int_e\left[\left(\{N\}^T\{\epsilon_x'\}_e\right)\{N\}\{N\}^T - \frac{d\{N\}}{d\bar{y}}\frac{d\{N\}^T}{d\bar{y}}\right]d\bar{y} \tag{5b}$$

$$[M] = \sum_e\int_e\{N\}\{N\}^T\,d\bar{y} \tag{5c}$$

$$\{\bar{E}_x\} = \sum_e\{\bar{E}_x\}_e \tag{5d}$$

$$\bar{y} = k_0y \tag{5e}$$

where ϵ_x' is expanded as

$$\epsilon_x' = \{N\}^T\{\epsilon_x'\}_e \tag{5f}$$

$$\{\epsilon_x'\}_e = \left[\epsilon_{x,1}' \quad \epsilon_{x,2}' \quad \epsilon_{x,3}'\right]^T \tag{5g}$$

and the boundary term associated with the first term of the left-hand side of (4) is dropped owing to the asymptotic conditions: $E_x = dE_x/dy = 0$ as $y \to \pm\infty$. The explicit forms of element matrices necessary for computing (5b) and (5c) are given in the Appendix.

The total guided wave power per unit length along the x axis is evaluated as

$$P = \frac{1}{2}\int_{-\infty}^{+\infty}E_xH_y^*\,dy = \frac{1}{2Z_0}\frac{\beta}{k_0}\int_{-\infty}^{+\infty}|E_x|^2\,dy \tag{6}$$

where * denotes the complex conjugate and Z_0 is the intrinsic impedance of a vacuum ($Z_0 = 377\ \Omega$).

To obtain ϵ_x' via (1a), it is necessary to compute the actual electric field E_x without normalization. The relation between the actual (E_x) and the normalized ($\bar{E}_x$) fields can be written as

$$|E_x| = \eta|\bar{E}_x| \tag{7}$$

where η is a scale factor. Substituting (5e) and (7) into (6), η is obtained:

$$\eta = \sqrt{4\pi Z_0\lambda_0^{-1}(\beta/k_0)^{-1}P}, \qquad \lambda_0 = 2\pi/k_0 \tag{8a}$$

where the usual normalization procedure of the eigenvector of (5a),

$$\int_{-\infty}^{+\infty}|\bar{E}_x|^2\,d\bar{y} = 1 \tag{8b}$$

is considered.

Equation (5a) is a nonlinear generalized eigenvalue problem whose eigenvalue and eigenvector correspond to $(\beta/k_0)^2$ and $\{\bar{E}_x\}$, respectively. Hence, one can solve it self-consistently using the following iterative scheme:

(i) Specify n, $\bar{n}$, λ_0, t, and P as input data and calculate the coefficient matrix $[M]$.

(ii) Assign initial values to β/k_0 and $\{\bar{E}_x\}$ in an arbitrary way. A convenient way to choose these

values is to use those for the linear case, i.e., $\epsilon_x' = \epsilon$ in (1a); we adopt this way in the present paper.

(iii) To obtain the nonlinear coefficient matrix $[K(E_x)]$, calculate η, $\{E_x\}$, and ϵ_x' sequentially.

(iv) To obtain a new set of β/k_0 and $\{\bar{E}_x\}$, solve the matrix eigenvalue equation (5a).

(v) Iterate the above procedures (iii) and (iv) until the solution (eigenvalue) converges within the desired criterion.

B. TM Waves (P-Polarized Waves).

We consider the following nonlinear relative permittivities ϵ_y' and ϵ_z' for TM polarization [4], [23]:

$$\epsilon_y' = \epsilon + af(E_y) + bf(E_z) \tag{9a}$$

$$\epsilon_z' = \epsilon + bf(E_y) + af(E_z) \tag{9b}$$

where the value of b depends on the particular nonlinear mechanism. For example, for electronic nonlinearities $b = a/3$, whereas for electrostrictive nonlinearities $b = a$ [23].

Substituting (9a) and (9b) into Maxwell's equations, the following nonlinear Helmholtz-type equation is derived:

$$\frac{d}{dy}\left(\frac{1}{\epsilon_z'}\frac{dH_x}{dy}\right) + \left(k_0^2 - \frac{\beta^2}{\epsilon_y'}\right)H_x = 0 \tag{10}$$

where the factor $\exp\{j(\omega t - \beta z)\}$ is implied.

Dividing the cross section along the y axis of the guide ($y \geq 0$) into a number of second-order line elements, the normalized magnetic fields within each element are defined in terms of those at the nodal points:

$$\bar{H}_x = \{N\}^T\{\bar{H}_x\}_e \tag{11a}$$

$$\{\bar{H}_x\}_e = \left[\bar{H}_{x,1} \quad \bar{H}_{x,2} \quad \bar{H}_{x,3}\right]^T \tag{11b}$$

where $\{\bar{H}_x\}_e$ is a magnetic field vector corresponding to the nodal points within each element.

Using Galerkin's procedure on a normalized version of (10) and integrating by parts, we obtain

$$\{N\}\frac{1}{\epsilon_z'}\frac{d\bar{H}_x}{dy}\bigg|_{y=y_1}^{y=y_2} - \int_{y_1}^{y_2}\frac{d\{N\}}{dy}\frac{1}{\epsilon_z'}\frac{d\bar{H}_x}{dy}\,dy + k_0^2\int_{y_1}^{y_2}\{N\}\bar{H}_x\,dy - \beta^2\int_{y_1}^{y_2}\frac{1}{\epsilon_y'}\{N\}\bar{H}_x\,dy = \{0\}. \tag{12}$$

Substituting (11a) into (12) and assembling the complete matrices for the system by adding the contributions of all different elements, we obtain

$$[K(H_x)]\{\bar{H}_x\} - (\beta/k_0)^2[M(H_x)]\{\bar{H}_x\} = \{0\} \tag{13a}$$

$$[K(H_x)] = \sum_e \int_e \left[\{N\}\{N\}^T - \left(\{N\}^T\{1/\epsilon_z'\}_e\right)\cdot\frac{d\{N\}}{d\bar{y}}\frac{d\{N\}^T}{d\bar{y}}\right]d\bar{y} \tag{13b}$$

$$[M(H_x)] = \sum_e \int_e \left(\{N\}^T\{1/\epsilon_y'\}_e\right)\{N\}\{N\}^T d\bar{y} \tag{13c}$$

$$\{\bar{H}_x\} = \sum_e \{\bar{H}_x\}_e \tag{13d}$$

where $1/\epsilon_i'$ $(i = y, z)$ is expanded as

$$1/\epsilon_i' = \{N\}^T\{1/\epsilon_i'\}_e \tag{13e}$$

$$\{1/\epsilon_i'\}_e = \left[1/\epsilon_{i,1}' \quad 1/\epsilon_{i,2}' \quad 1/\epsilon_{i,3}'\right]^T \tag{13f}$$

and the boundary term associated with the first term of the left-hand side of (12) is dropped owing to the asymptotic conditions: $H_x = dH_x/dy = 0$ as $y \to \pm\infty$. The explicit forms of element matrices necessary for computing (13b) and (13c) are given in the Appendix.

The total guided wave power per unit length along the x axis is evaluated as

$$P = -\frac{1}{2}\int_{-\infty}^{+\infty} E_y H_x^*\,dy = \frac{Z_0}{2}\frac{\beta}{k_0}\int_{-\infty}^{+\infty}\frac{1}{\epsilon_y'}|H_x|^2\,dy. \tag{14}$$

To obtain ϵ_y' and ϵ_z' via (9a) and (9b), respectively, it is necessary to compute the actual magnetic field H_x without normalization. The relation between the actual (H_x) and the normalized ($\bar{H}_x$) fields can be written as

$$|H_x| = \xi|\bar{H}_x| \tag{15}$$

where ξ is a scale factor. Substituting (5e) and (15) into (14), ξ is obtained:

$$\xi = \sqrt{4\pi Z_0^{-1}\lambda_0^{-1}(\beta/k_0)^{-1}P} = \eta/Z_0 \tag{16a}$$

where the usual normalization procedure of the eigenvector of (13a),

$$\int_{-\infty}^{+\infty}\frac{1}{\epsilon_y'}|\bar{H}_x|^2\,d\bar{y} = 1 \tag{16b}$$

is considered.

Once H_x is obtained, the actual electric-field components E_y and E_z necessary to evaluate ϵ_y' and ϵ_z' via (9a) and (9b), respectively, can be straightforwardly derived with the help of Maxwell's equations:

$$E_y = -Z_0\frac{\beta}{k_0}\frac{1}{\epsilon_y'}H_x \tag{17a}$$

$$E_z = jZ_0\frac{1}{\epsilon_z'}\frac{dH_x}{d\bar{y}}. \tag{17b}$$

With these relations, the nodal electric field vectors for E_y and E_z can be computed as

$$\{E_y\} = -Z_0\frac{\beta}{k_0}\left[\frac{H_{x,1}}{\epsilon_{y,1}'} \quad \frac{H_{x,2}}{\epsilon_{y,2}'} \quad \frac{H_{x,3}}{\epsilon_{y,3}'}\right]^T \tag{18a}$$

$$\{E_z\} = \frac{jZ_0}{\bar{l}}\left[\frac{F_1}{\epsilon_{z,1}'} \quad \frac{F_2}{\epsilon_{z,2}'} \quad \frac{F_3}{\epsilon_{z,3}'}\right]^T \tag{18b}$$

where

$$\bar{l} = \bar{y}_2 - \bar{y}_1 = k_0 l \tag{18c}$$

$$F_1 = -3H_{x,1} - H_{x,2} + 4H_{x,3} \tag{18d}$$

$$F_2 = H_{x,1} + 3H_{x,2} - 4H_{x,3} \tag{18e}$$

$$F_3 = -H_{x,1} + H_{x,2}. \tag{18f}$$

Equation (13a) is a nonlinear generalized eigenvalue problem whose eigenvalue and eigenvector correspond to

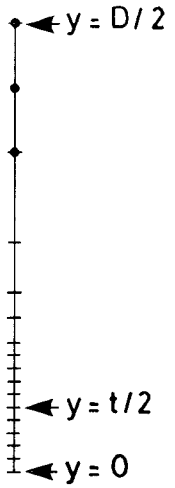

Fig. 2. Element division for the system of Fig. 1. The upper half of the waveguide cross section is subdivided into 15 line elements; the number of nodal points is 31.

$(\beta/k_0)^2$ and $\{\overline{H}_x\}$, respectively. Hence, one can solve it self-consistently using the following iterative scheme:

(i) Specify n, $\bar{n}$, λ_0, t, and P as input data.
(ii) Assign initial values to β/k_0 and $\{\overline{H}_x\}$ in an arbitrary way. As with TE waves, a way to choose these values is to use those for the linear case, i.e., $\epsilon_y' = \epsilon_z' = \epsilon$ in (9a) and (9b); we adopt this way in the present paper.
(iii) To obtain the nonlinear coefficient matrices $[K(H_x)]$ and $[M(H_x)]$, calculate ξ, $\{H_x\}$, $\{E_y\}$, $\{E_z\}$, ϵ_y', and ϵ_z' sequentially.
(iv) To obtain a new set of β/k_0 and $\{\overline{H}_x\}$, solve the matrix eigenvalue equation (13a).
(v) Iterate the above procedures (iii) and (iv) until the solution converges within the desired criterion.

Note that in the present modeling the nonlinear permittivities are given by (9a) and (9b); therefore, the biaxial nature of nonlinear material for TM-polarized waves is considered without any approximate treatment such as uniaxial approximations [7], [9], [12], [13], [25], [26].

III. Numerical Examples and Discussion

We consider a linear thin film ($|y| \leqslant t/2$) bounded by two identical nonlinear claddings. As a nonlinear material, we concentrate on the liquid crystal MBBA [8], [11], [29] because of its very large nonlinearity. Preliminary experiments [29] with it have shown evidence for nonlinear guided waves. The waveguide parameters [8], [11] are $n_1 = n_3 = 1.55$, $n_2 = 1.57$, $\bar{n}_1 = \bar{n}_3 = 10^{-9}$ m^2/W (self-focusing action), $\bar{n}_2 = 0$, and the wavelength is 0.515 μm (Ar^+ laser). As the $f(E_i)$ $(i = x, y, z)$ in (1a), (9a), and (9b), we consider a power-law nonlinearity defined by [18],

$$f(E_i) = |E_i|^\alpha \qquad (i = x, y, z) \tag{19}$$

where α is a positive parameter representing a variety of nonlinearities. For the Kerr-like nonlinearity, $\alpha = 2$. Although asymmetric modes [11], [14] can exist in nonlinear waveguides even for symmetric configurations, we concentrate solely on the symmetric or antisymmetric mode in what follows.

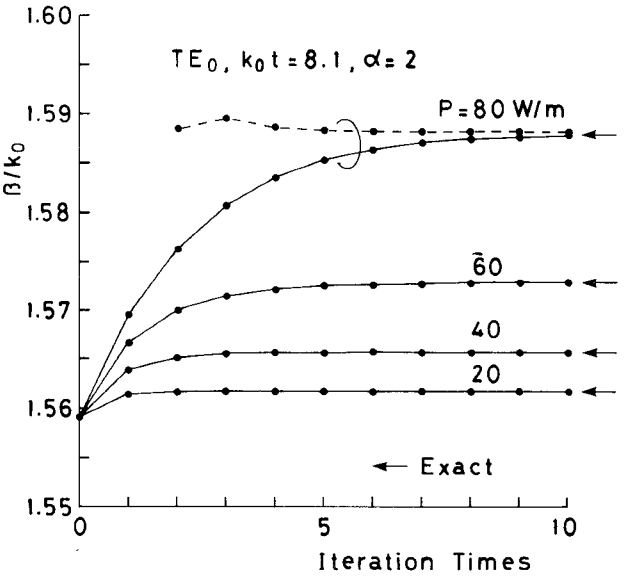

(a)

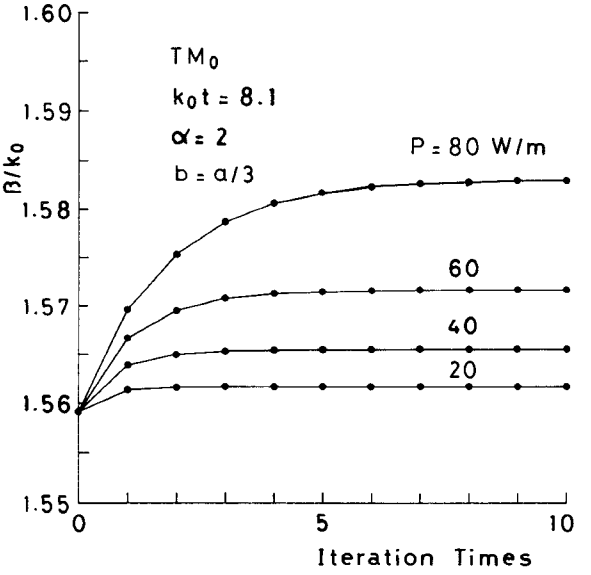

(b)

Fig. 3. Convergence behavior of effective refractive index. The solid lines are of simple iteration, whereas the broken line is of the Aitken method. (a) TE_0 mode. (b) TM_0 mode.

The division profile used is illustrated in Fig. 2, where only the upper half of the guide is considered because of the symmetry nature of the system and the field distribution. On $y = D/2$ $(D = 7t)$, the Dirichlet-type boundary condition, i.e., $E_x = 0$ for TE mode and $H_x = 0$ for TM mode, is imposed because we consider the waves trapped in a film or the vicinity of it.

First, to confirm the validity of the present algorithm, we examine the convergence behavior of solutions versus iteration times. Fig. 3 demonstrates the convergence of the effective refractive index, taking the total optical power as a parameter. Stable and monotonic convergence is ob-

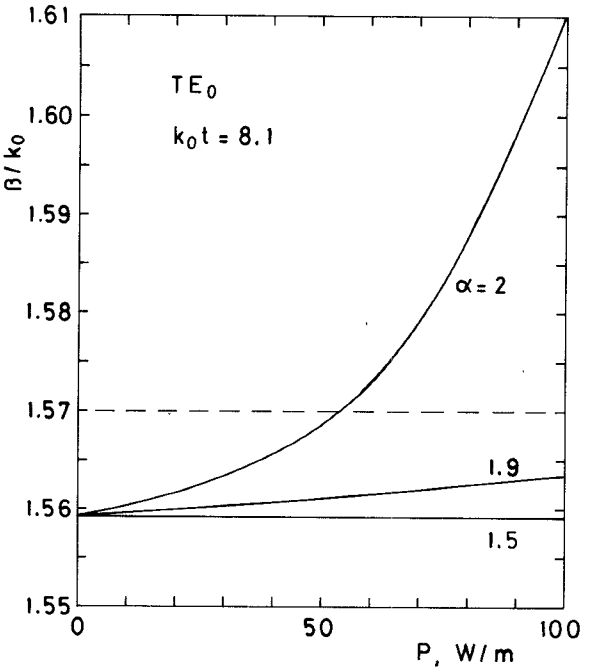

(a)

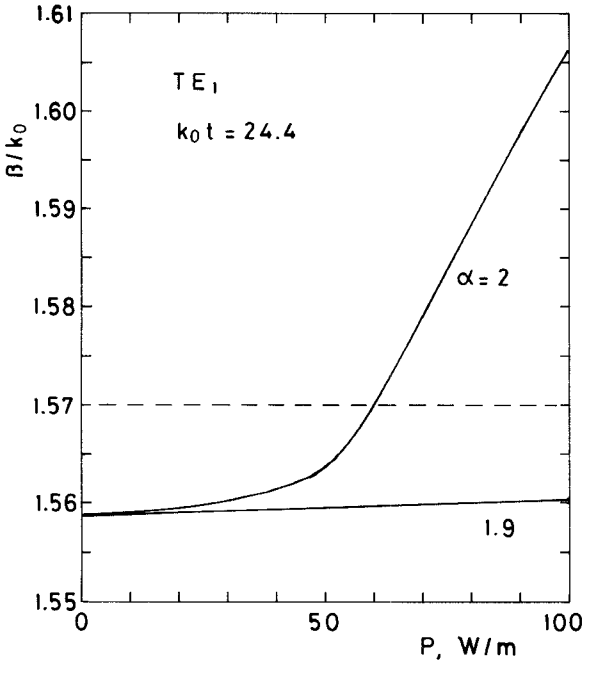

(b)

Fig. 4. Dependence of effective refractive index on total optical power for power-law nonlinearity. The Kerr-like nonlinearity corresponds to $\alpha = 2$. (a) TE_0 mode. (b) TE_1 mode.

served for both polarizations. Since exact analytical solutions are available for TE waves, we compare in Fig. 3(a) our numerical results with exact ones [11]. It is seen from Fig. 3(a) that the solution converges to the exact value in both the guided-wave ($n_1 < \beta/k_0 < n_2$) and the surface-wave ($\beta/k_0 > n_2$) regions.

Although a simple iterative scheme without any acceleration is applied in Fig. 3, it is efficient to utilize skillful techniques that can accelerate convergence speed. One of

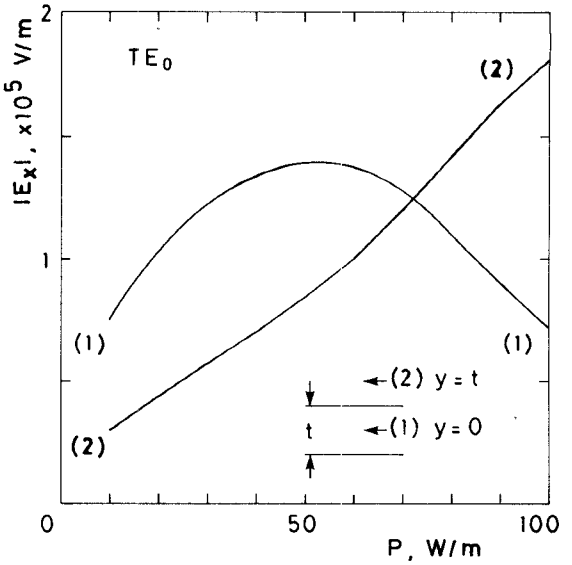

Fig. 5. Variation of local electric field strength as a function of total optical power ($k_0 t = 8.1$, $\alpha = 2$).

straightforward ways for acceleration is the Aitken method, whose algorithm is as follows [30]:

$$s'_m = s_m - \frac{(s_m - s_{m-1})^2}{s_m - 2s_{m-1} + s_{m-2}} \qquad (m = 2,3,4,\cdots) \quad (20)$$

where $\{s_m\}$ is a sequence of numbers composed of solutions under iteration. The new sequence of numbers, $\{s'_m\}$, is expected to converge faster than the original one. An example of the effect of this technique is shown in Fig. 3(a) with a broken line for $P = 80$ W/m. Comparison between the solid and broken lines successfully demonstrates the usefullness of the technique.

Fig. 4 shows the dependence of the effective refractive index on total optical power for TE modes. It is seen from Fig. 4 that for Kerr-like media, $\alpha = 2$, the guided wave changes into a surface wave at a certain power level. This phenomenon is peculiar to nonlinear waveguides and has no linear counterpart [11]. Furthermore, it is very interesting to note that the characteristic is drastically changed by a slight deviation from the Kerr-like nonlinearity. This phenomenon is due to the fact that the threshold power, which is defined by the total optical power for $\beta/k_0 = 1.57$, increases sensitively with decreasing α. This suggests that the details of the nonlinearity are very important for designing nonlinear integrated optics devices.

One of many fascinating features of nonlinear waveguides is the flux-dependent behavior of a field distribution. Fig. 5 shows the dependence of local electric field strength on total optical power for $\alpha = 2$ in Fig. 4(a). In the range of low power level, the strength at the center ($y = 0$) of the film is larger than that at $y = t$ in the cladding, and both of them increase with increasing power. However, in the range of high power level, the dominance of field strength is reversed, and the strength at the center decreases with increasing power, whereas that at $y = t$ still increases. This characteristic indicates that the wave evolves

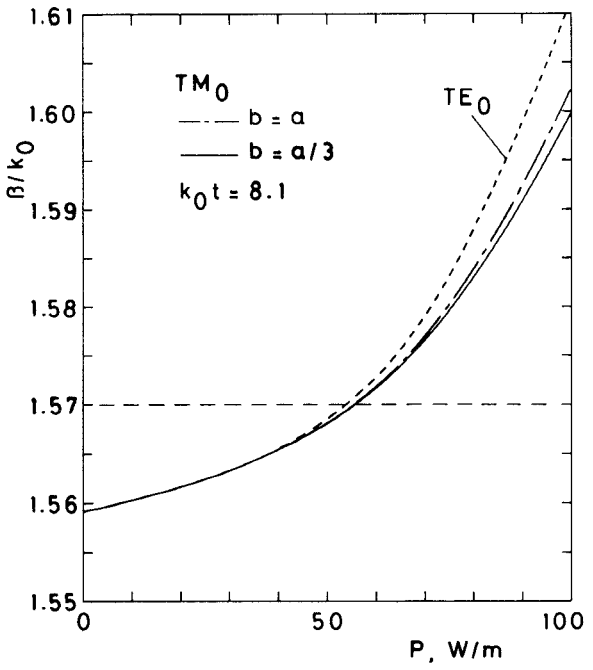

(a)

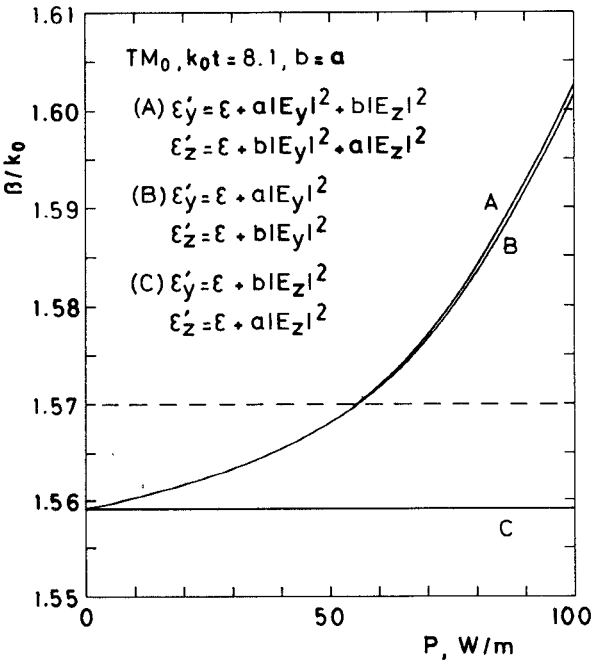

(b)

Fig. 6. Dependence of effective refractive index on total optical power for TM_0 mode. (a) Comparison with TE_0 mode. (b) Comparison with approximate procedures.

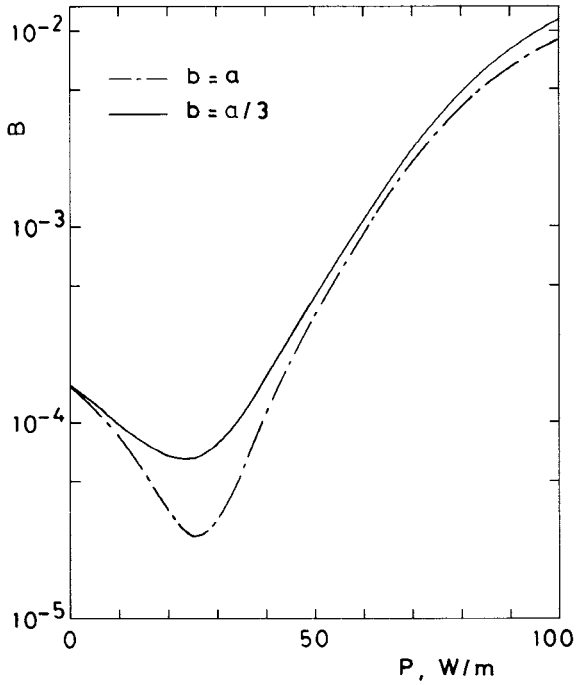

Fig. 7. Modal birefringence versus total optical power.

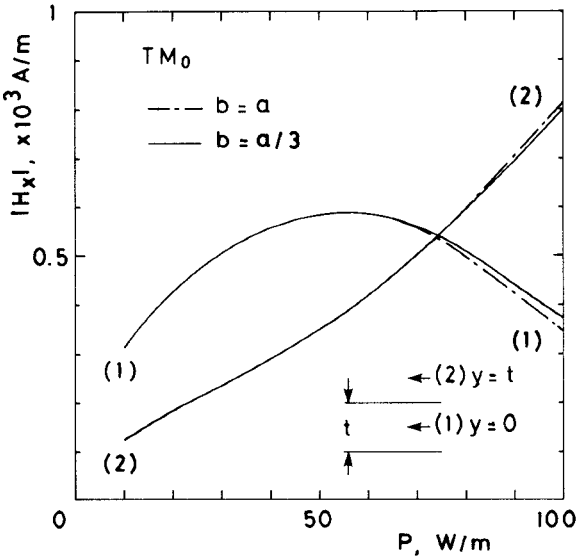

Fig. 8. Variation of local magnetic field strength as a function of total optical power.

into a single interface surface polariton [4], [5] as the optical flux density increases.

Numerical results for TM polarization are shown in Figs. 6–8, where $\alpha = 2$ and $k_0 t = 8.1$. Fig. 6(a) shows the dependence of the effective refractive indices on total optical power for the electrostrictive ($b = a$) and electronic ($b = a/3$) nonlinearities and compares it with that of the TE counterpart. Characteristics similar to the TE mode are found for the TM mode, particularly in the guided-wave region.

Fig. 6(b) compares the results for the permittivities given by (9a) and (9b) (case A) with those for two approximate models (cases B and C) in which nonlinear permittivities are assumed to depend solely on one of two nonzero electric-field components. Since $|E_z| \ll |E_y|$ in the present configuration, case B gives far more accurate results than case C. Again, it is evident from this investigation that the appropriate modeling for the nonlinearity is very important for predicting intensity-dependent properties of nonlinear guided-wave devices.

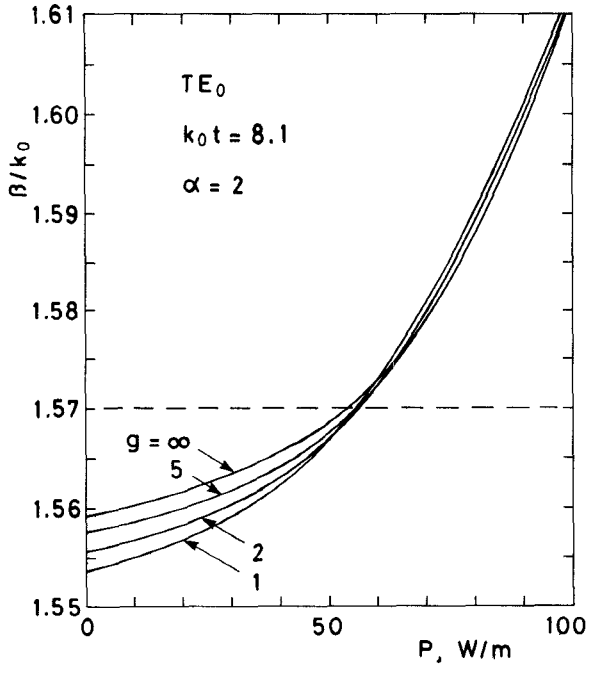

Fig. 9. Effect of film index profiles on dispersion relations.

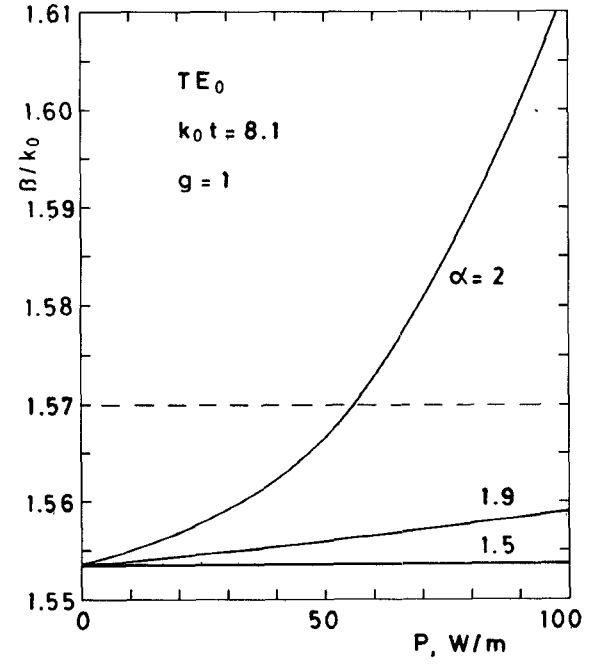

Fig. 10. Dependence of effective refractive index on total optical power for triangular profile.

Fig. 7 exhibits the modal birefringence B versus total optical power. B is defined by

$$B = (\beta_{TE} - \beta_{TM})/k_0 \tag{21}$$

where β_{TE} and β_{TM} are the phase constants of the TE_0 and TM_0 modes, respectively. For both types of nonlinearities, a minimum of the birefringence is observed at $P \simeq 25$ W/m. Above this point, the value of the modal birefringence is greatly enhanced with increasing optical power.

Fig. 8 shows the dependence of local magnetic field strength on total optical power. The same characteristics are found as for the TE wave shown in Fig. 5.

Up to now, we have confined ourselves to a film with a homogeneous refractive-index distribution. In what follows, we apply the present method to nonlinear waveguides with inhomogeneous index profiles and investigate the relation between the refractive-index profile and the characteristics. We consider here the following g-power function as a refractive-index profile in the film:

$$\epsilon(y) = n^2(y) = n_1^2 + (n_2^2 - n_1^2)(1 - |2y/t|^g) \quad (|y| \leq t/2) \tag{22}$$

where g is a positive parameter representing distributions; the homogeneous profile corresponds to $g = \infty$.

Fig. 9 shows an example of numerical results. It is found from Fig. 9 that the behavior in the surface-wave region is similar irrespective of g.

Fig. 10 examines the effective index versus total optical power for triangular profile ($g = 1$). Just as in the step profile (Fig. 4(a)), the characteristic is drastically changed by a slight decrease in α.

IV. Conclusions

We have proposed a general-purpose approach based on the finite-element method for analyzing optical waves guided by dielectric slab waveguides with arbitrary nonlinear media and with arbitrary refractive-index distribution. Using this approach, we have solved several kinds of waveguides that include non-Kerr-like media and an inhomogeneous film. For these realistic cases, the conventional analytical approach is of little use. The most useful feature of the present method is that it can treat TM waves without any approximation for nonlinear permittivities.

Although we have concentrated solely on the symmetric (or antisymmetric) mode and the single-valued propagation constant, one can apply the present method also to the asymmetric mode and the multivalued propagation constant frequently observed in high-frequency (large $k_0 t$) cases [8], [11], [14], [19], [21], [27] provided that the initial value of the iteration is taken appropriately. Application of the present scheme to these cases will be made in future.

Appendix
The Explicit Forms of Element Matrices

The explicit forms of element matrices involving in (5b), (5c), (13b), and (13c) in the text are given by

$$\int_e \frac{d\{N\}}{d\bar{y}} \frac{d\{N\}^T}{d\bar{y}} d\bar{y} = \frac{1}{3\bar{l}} \begin{bmatrix} 7 & 1 & -8 \\ 1 & 7 & -8 \\ -8 & -8 & 16 \end{bmatrix} \tag{A1}$$

$$\int_e \{N\}\{N\}^T d\bar{y} = \frac{\bar{l}}{30} \begin{bmatrix} 4 & -1 & 2 \\ -1 & 4 & 2 \\ 2 & 2 & 16 \end{bmatrix} \tag{A2}$$

$$\int_e \left(\{N\}^T\{q\}_e\right)\frac{d\{N\}}{d\bar{y}}\frac{d\{N\}^T}{d\bar{y}}\,d\bar{y}=\frac{1}{\bar{l}}\begin{bmatrix}s_{11}&s_{12}&s_{13}\\s_{12}&s_{22}&s_{23}\\s_{13}&s_{23}&s_{33}\end{bmatrix} \tag{A3a}$$

$$s_{11}=\frac{37}{30}q_1-\frac{1}{10}q_2+\frac{6}{5}q_3 \tag{A3b}$$

$$s_{12}=\frac{7}{30}q_1+\frac{7}{30}q_2-\frac{2}{15}q_3 \tag{A3c}$$

$$s_{13}=-\frac{22}{15}q_1-\frac{2}{15}q_2-\frac{16}{15}q_3 \tag{A3d}$$

$$s_{22}=-\frac{1}{10}q_1+\frac{37}{30}q_2+\frac{6}{5}q_3 \tag{A3e}$$

$$s_{23}=-\frac{2}{15}q_1-\frac{22}{15}q_2-\frac{16}{15}q_3 \tag{A3f}$$

$$s_{33}=\frac{8}{5}q_1+\frac{8}{5}q_2+\frac{32}{15}q_3 \tag{A3g}$$

$$\int_e \left(\{N\}^T\{q\}_e\right)\{N\}\{N\}^T d\bar{y}=\bar{l}\begin{bmatrix}m_{11}&m_{12}&m_{13}\\m_{12}&m_{22}&m_{23}\\m_{13}&m_{23}&m_{33}\end{bmatrix} \tag{A4a}$$

$$m_{11}=\frac{13}{140}q_1-\frac{1}{140}q_2+\frac{1}{21}q_3 \tag{A4b}$$

$$m_{12}=-\frac{1}{140}q_1-\frac{1}{140}q_2-\frac{2}{105}q_3 \tag{A4c}$$

$$m_{13}=\frac{1}{21}q_1-\frac{2}{105}q_2+\frac{4}{105}q_3 \tag{A4d}$$

$$m_{22}=-\frac{1}{140}q_1+\frac{13}{140}q_2+\frac{1}{21}q_3 \tag{A4e}$$

$$m_{23}=-\frac{2}{105}q_1+\frac{1}{21}q_2+\frac{4}{105}q_3 \tag{A4f}$$

$$m_{33}=\frac{4}{105}q_1+\frac{4}{105}q_2+\frac{16}{35}q_3 \tag{A4g}$$

where $\bar{l}=k_0 l$, $\{q\}_e=[q_1 \quad q_2 \quad q_3]^T$, and the formula

$$\int_e L_1^i L_2^j\,d\bar{y}=\frac{i!j!}{(i+j+1)!}\bar{l} \qquad (i, j: \text{nonnegative integers}) \tag{A5}$$

has been used.

Acknowledgment

The authors would like to express their gratitude to the late Professor Michio Suzuki of Hokkaido University for his advice and encouragement during his lifetime. They would also like to thank Dr. Y. Satomura of Osaka Institute of Technology for helpful discussions and Dr. M. Miyagi of Tohoku University for sending them reprints of his work.

References

[1] T E. Rozzi, "Modal analysis for nonlinear processes in optical and quasi-optical waveguides," *IEEE J. Quantum Electron.*, vol. QE-6, pp. 539–546, Sept. 1970.

[2] M. Miyagi and S. Nishida, "Guided waves in bounded nonlinear medium (II)–dielectric boundaries–," *Sci. Rep. Res. Inst. Elect. Commun., Tohoku Univ.*, vol. 24, pp. 53–67, 1972.

[3] M. Miyagi and S. Nishida, "Surface waves along nonlinear dielectric slab," *Trans. Inst. Electron. Commun. Eng. Japan*, vol. 58-C, pp. 363–369, July 1975 (in Japanese).

[4] A. A. Maradudin, "Nolinear surface electromagnetic waves," in *Optical and Acoustic Waves in Solids — Modern Topics*, M. Borissov, Ed. Singapore: World Scientific Publ., 1983, pp. 72–142.

[5] G. I. Stegeman, C. T. Seaton, W. M. Hetherington III, A. D Boardman, and P. Egan, "Nonlinear guided waves," in *Nonlinear Optics: Materials and Devices*, C. Flytzanis and J. L. Oudar, Eds. Berlin and Heidelberg: Springer-Verlag, 1986, pp. 31–64.

[6] G. I. Stegeman, "Guided wave approaches to optical bistability," *IEEE J. Quantum Electron.*, vol. QE-18, pp. 1610–1619, Oct. 1982

[7] U. Langbein, F. Lederer, and H-E. Ponath, "A new type of nonlinear slab-guided waves," *Opt. Commun.*, vol. 46, pp. 167–169, July 1983.

[8] G. I Stegeman, C. T. Seaton, J. Chilwell, and S. D. Smith, "Nonlinear waves guided by thin films," *Appl. Phys. Lett.*, vol. 44, pp. 830–832, May 1984.

[9] C. T. Seaton, J. D. Velera, B. Svenson, and G. I. Stegeman, "Comparison of solutions for TM-polarized nonlinear guided waves," *Opt. Lett.*, vol. 10, pp. 149–150, Mar. 1985.

[10] U. Langbein, F. Lederer, and H.-E. Ponath, "Generalized dispersion relations for nonlinear slab-guided waves," *Opt. Commun.*, vol. 53, pp. 417–420, Apr. 1985.

[11] C. T. Seaton, J. D. Valera, R. L. Shvemaker, G. I. Stegeman, J. T. Chilwell, and S. D. Smith, "Calculations of nonlinear TE waves guided by thin dielectric films bounded by nonlinear media," *IEEE J. Quantum Electron.*, vol. QE-21, pp. 774–783, July 1985.

[12] G. I. Stegeman, C. T. Seaton, and J. Ariyasu, "Nonlinear electromagnetic waves guided by a single interface," *J. Appl. Phys.*, vol. 58, pp. 2453–2459, Oct. 1985.

[13] J. Ariyasu, C. T. Seaton, and G. I. Stegeman, "Nonlinear surface polaritons guided by metal films," *J. Appl. Phys.*, vol. 58, pp. 2460–2466, Oct. 1985.

[14] A. D. Boardman and P. Egan, "S-polarized waves in a thin dielectric film asymmetrically bounded by optically nonlinear media," *IEEE J. Quantum Electron.*, vol. QE-21, pp. 1701–1713, Oct. 1985.

[15] U. Langbein, F. Lederer, T. Peschel, and H.-E. Ponath, "Nonlinear guided waves in saturable nonlinear media," *Opt. Lett.*, vol. 10, pp. 571–573, Nov. 1985.

[16] A. D. Boardman and P. Egan, "Optically nonlinear waves in thin films," *IEEE J. Quantum Electron.*, vol. QE-22, pp. 319–324, Feb. 1986.

[17] J. V. Moloney, J. Ariyasu, C. T. Seaton, and G. I. Stegeman, "Numerical evidence for nonstationary, nonlinear, slab-guided waves," *Opt. Lett.*, vol. 11, pp. 315–317, May 1986.

[18] G. I. Stegeman, E. M. Wright, C. T. Seaton, J. V. Moloney, T.-P. Shen, A. A. Maradudin, and R. F. Wallis, "Nonlinear slab-guided waves in non-Kerr-like media," *IEEE J. Quantum Electron.*, vol. QE-22, pp. 977–983, June 1986.

[19] Y. Satomura, "Propagation of nonlinear waves in dielectric optical waveguide," *Tech. Res. Rep. Inst. Electron. Commun. Eng. Japan*, vol. OCT86-24, pp. 74–79, Aug. 1986 (in Japanese).

[20] L. Leine, Ch. Wachter, U. Langbein, and F. Lederer, "Propagation phenomena of nonlinear film-guided waves: a numerical analysis," *Opt. Lett.*, vol. 11, pp. 590–592, Sept. 1986.

[21] R. K. Varshney, M. A. Nehme, R. Srivastava, and R. V. Ramaswamy, "Guided waves in graded-index planar waveguides with nonlinear cover medium," *Appl. Opt.*, vol. 25, pp. 3899–3902, Nov. 1986.

[22] W. R. Holland, "Nonlinear guided waves in low-index, self-focusing thin films: transverse electric case," *J. Opt. Soc. Amer. B*, vol. 3, pp. 1529–1534, Nov. 1986.

[23] D. Mihalache, G. I. Stegeman, C. T. Seaton, E. M. Wright, R. Zanoni, A. D. Boardman, and T. Twardowski, "Exact dispersion relations for transverse magnetic polarized guided waves at a nonlinear interface," *Opt. Lett.*, vol. 12, pp. 187–189, Mar. 1987.

[24] K. Hayata, M. Koshiba, and M. Suzuki, "Finite-element solution of arbitrarily nonlinear, graded-index slab waveguides," *Electron. Lett.*, vol. 23, pp. 429–431, Apr. 1987.

[25] A. Kumar and M. S. Sodha, "Transverse-magnetic-polarized nonlinear modes guided by a symmetric five-layer dielectric structure," *Opt. Lett.*, vol. 12, pp. 352–354, May 1987.
[26] Y. Satomura, "Propagation of nonlinear TM waves in dielectric optical waveguide," in *Proc. Sino-Japanese Joint Meeting on Optical Fiber Sci. and Electromagn. Theory* (Nanjing, China), May 1987, pp. 291–296.
[27] Y. Satomura, "Propagation characteristics of nonlinear TE waves in dielectric optical waveguide with nonlinear media," *Trans. Inst. Electron. Inform. Commun. Eng.*, vol. E70, pp. 541–543, June 1987.
[28] K. Hayata, M. Nagai, and M. Koshiba, "Finite-element theory of nonlinear TM-polarised guided waves," *Electron. Lett.*, vol. 23, pp. 1305–1307, Nov. 1987.
[29] H. Vach, C. T. Seaton, G. I. Stegeman, and I. C. Khoo, "Observation of intensity-dependent guided waves," *Opt. Lett.*, vol. 9, pp. 238–240, June 1984.
[30] P. Henrici, *Elements of Numerical Analysis*. New York: Wiley, 1964.

Kazuya Hayata was born in Kushiro, Japan, on December 1, 1959. He received the B.S. and M.S. degrees in electronic engineering from Hokkaido University, Sapporo, Japan, in 1982 and 1984, respectively.

Since 1984, he has been an Instructor of Electronic Engineering at Hokkaido University. He has been engaged in research on guided-wave optics, microwave theory and techniques, computational mechanics for field problems, quantum-wave electronics, and surface acoustic waves.

Mr. Hayata is a member of the Institute of Electronics, Information and Communication Engineers (IEICE), the Japan Society of Applied Physics (JSAP), the Optics Division in the JSAP, and the Optical Society of America. In 1987, he was awarded the 1986 Excellent Paper Award by the IEICE.

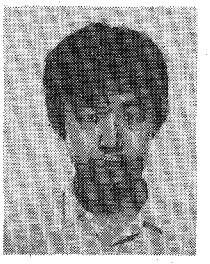

Michio Nagai was born in Sapporo, Japan, on July 25, 1964. He received the B.S. degree in electronic engineering from Hokkaido University, Sapporo, Japan, in 1987. He is presently studying toward the M.S. degree in electronic engineering at Hokkaido University.

Mr. Nagai is a member of the Institute of Electronics, Information and Communication Engineers.

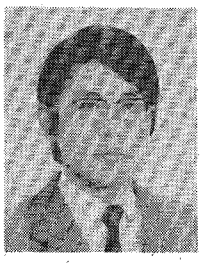

Masanori Koshiba (SM'84) was born in Sapporo, Japan, on November 23, 1948. He received the B.S., M.S., and Ph.D. degrees in electronic engineering from Hokkaido University, Sapporo, Japan, in 1971, 1973, and 1976, respectively.

In 1976, he joined the Department of Electronic Engineering, Kitami Institute of Technology, Kitami, Japan. From 1979 to 1987, he was an Associate Professor of Electronic Engineering at Hokkaido University, and in 1987 he became a Professor. He has been engaged in research on lightwave technology, surface acoustic waves, magnetostatic waves, microwave field theory, and applications of finite-element and boundary-element methods to field problems.

Dr. Koshiba is a member of the Institute of Electronics, Information and Communication Engineers (IEICE), the Institute of Television Engineers of Japan, the Institute of Electrical Engineers of Japan, the Japan Society for Simulation Technology, and the Japan Society for Computational Methods in Engineering. In 1987, he was awarded the 1986 Excellent Paper Award by the IEICE.